



Early-Stage White Matter Lesions Detected by Multispectral MRI Segmentation Predict Progressive Cognitive Decline

Hanna Jokinen^{1*}, Nicolau Gonçalves², Ricardo Vigário^{2,3}, Jari Lipsanen⁴, Franz Fazekas⁵, Reinhold Schmidt⁵, Frederik Barkhof⁶, Sofia Madureira⁷, Ana Verdelho⁷, Domenico Inzitari⁸, Leonardo Pantoni⁸, Timo Erkinjuntti¹ and the LADIS Study Group[†]

OPEN ACCESS

Edited by:

John Ashburner,
University College London, UK

Reviewed by:

Lei Wang,
Northwestern University Feinberg
School of Medicine, USA
Delia Cabrera DeBuc,
University of Miami, USA

*Correspondence:

Hanna Jokinen
hanna.jokinen@helsinki.fi

[†]The collaborators of the LADIS study
are listed in the Supplementary
Materials (Appendix II).

Specialty section:

This article was submitted to
Brain Imaging Methods,
a section of the journal
Frontiers in Neuroscience

Received: 26 June 2015

Accepted: 16 November 2015

Published: 02 December 2015

Citation:

Jokinen H, Gonçalves N, Vigário R,
Lipsanen J, Fazekas F, Schmidt R,
Barkhof F, Madureira S, Verdelho A,
Inzitari D, Pantoni L, Erkinjuntti T and
the LADIS Study Group (2015)
Early-Stage White Matter Lesions
Detected by Multispectral MRI
Segmentation Predict Progressive
Cognitive Decline.
Front. Neurosci. 9:455.
doi: 10.3389/fnins.2015.00455

¹ Clinical Neurosciences, Neurology, University of Helsinki and Helsinki University Hospital, Helsinki, Finland, ² Department of Information and Computer Science, Aalto University School of Science, Espoo, Finland, ³ Department of Physics, University Nova of Lisbon, Lisbon, Portugal, ⁴ Institute of Behavioural Sciences, University of Helsinki, Helsinki, Finland, ⁵ Department of Neurology and MRI Institute, Medical University of Graz, Graz, Austria, ⁶ Department of Radiology and Neurology, VU University Medical Center, Amsterdam, Netherlands, ⁷ Serviço de Neurologia, Centro de Estudos Egas Moniz, Hospital de Santa Maria, Lisbon, Portugal, ⁸ Department of Neurological and Psychiatric Sciences, University of Florence, Florence, Italy

White matter lesions (WML) are the main brain imaging surrogate of cerebral small-vessel disease. A new MRI tissue segmentation method, based on a discriminative clustering approach without explicit model-based added prior, detects partial WML volumes, likely representing very early-stage changes in normal-appearing brain tissue. This study investigated how the different stages of WML, from a “pre-visible” stage to fully developed lesions, predict future cognitive decline. MRI scans of 78 subjects, aged 65–84 years, from the Leukoaraiosis and Disability (LADIS) study were analyzed using a self-supervised multispectral segmentation algorithm to identify tissue types and partial WML volumes. Each lesion voxel was classified as having a small (33%), intermediate (66%), or high (100%) proportion of lesion tissue. The subjects were evaluated with detailed clinical and neuropsychological assessments at baseline and at three annual follow-up visits. We found that voxels with small partial WML predicted lower executive function compound scores at baseline, and steeper decline of executive scores in follow-up, independently of the demographics and the conventionally estimated hyperintensity volume on fluid-attenuated inversion recovery images. The intermediate and fully developed lesions were related to impairments in multiple cognitive domains including executive functions, processing speed, memory, and global cognitive function. In conclusion, early-stage partial WML, still too faint to be clearly detectable on conventional MRI, already predict executive dysfunction and progressive cognitive decline regardless of the conventionally evaluated WML load. These findings advance early recognition of small vessel disease and incipient vascular cognitive impairment.

Keywords: executive functions, cognition, image analysis, MRI, neuropsychology, white matter lesions, small vessel disease

INTRODUCTION

Cerebral small vessel disease (SVD) is the most common cause of vascular cognitive impairment and dementia. White matter lesions (WML) are the core marker of SVD on brain imaging, together with lacunar infarcts, microbleeds, and brain atrophy. All these findings have been shown to influence clinical and cognitive outcome (Jokinen et al., 2011, 2012; Muller et al., 2011; Poels et al., 2012). The Leukoaraiosis and Disability (LADIS) study, among other studies, has demonstrated that WML are related to cognitive decline, impaired functional abilities, depression, and gait and balance disturbances (LADIS Study Group, 2011).

Magnetic resonance imaging (MRI) has been the standard method in evaluating WML. Despite significant recent improvements in quantitative image analysis techniques, one of the major obstacles in MRI is still its finite spatial resolution, which leads to partial volume effects. Together with noise and inhomogeneity, it poses difficulties to brain segmentation techniques. Often, a careful analysis of the borders between healthy and pathological tissues is required to delineate the extent and severity of lesions, applying an implicit “decision-threshold” for lesion segmentation. Furthermore, hyperintensities in MRI seem to only represent the end-stage of the disease process. More widespread tissue damage may be associated with WML, not visible on routine MRI (Schmidt et al., 2011). There is no standard to evaluate such early stages of tissue damage, since their intensity values are not sufficiently distinct from those of normal tissues.

Most modern segmentation methods rely on prior information, such as average brain atlases (Smith et al., 2004; Ashburner and Friston, 2005; Goebel et al., 2006) or manual labeling (Wismüller et al., 2004; Lee et al., 2009; Cruz-Barbosa and Vellido, 2011). Recently, a new data-driven method for tissue segmentation has been proposed, based on a discriminative clustering (DC) strategy, in a self-supervised machine learning approach (Gonçalves et al., 2014). This method reduces the use of prior information to a minimum, and utilizes multispectral MRI data. Unlike other methods, targeting only healthy tissues (Pham and Prince, 1998; Van Leemput et al., 1999; Zhang et al., 2001; Manjón et al., 2010) or specific types of lesions (Van Leemput et al., 2001; Zijdenbos et al., 2002; Styner et al., 2008; Cruz-Barbosa and Vellido, 2011), DC allows for the study of a wide range of normal and abnormal tissue types. Another major asset of the proposed method is its ability to estimate tissue probabilities for each voxel, necessary for a suitable characterization of WML evolution. Voxels can be

categorized as containing small (still too faint to be clearly visible), intermediate or high proportion of WML. Those containing a small proportion of lesion are usually outside the “decision-threshold” of conventional segmentation, and point to early-stage WML.

The focus in the present study is to observe how the different stages of lesions are related to cognitive performance in a sample of elderly subjects with mild to moderate WML. The data used consisted of MRI measurements collected in a 3-year follow-up period, and annual neuropsychological assessments within that period. In particular, we were interested in determining whether even the earliest-stage small partial WML volumes, in normal-appearing brain tissue, are able to independently predict future cognitive decline, incremental to the conventionally evaluated WML load.

METHODS

Subjects and Design

The subjects were a subgroup of participants ($n = 78$) from three centers (Amsterdam $n = 21$, Graz $n = 18$, Helsinki $n = 39$) of the LADIS study, a European multicenter study investigating the impact of age-related WML in transition from functional independence into disability. The LADIS protocol and the sample characteristics have been reported in detail elsewhere (Pantoni et al., 2005). In short, 639 subjects were enrolled in 11 centers according to the following inclusion criteria: (a) age 65–84 years, (b) mild to severe WML according to the revised Fazekas scale (Pantoni et al., 2005), (c) no or minimal impairment in the Instrumental Activities of Daily Living scale (≤ 1 of 8 items compromised) (Lawton and Brody, 1969), and (d) presence of a regularly contactable informant. Exclusion criteria were: (a) severe illness likely prone to drop-out from follow-up (cardiac, hepatic, or renal failure, neoplastic, or other relevant systemic disease), (b) severe unrelated neurological illness or psychiatric disorder, (c) leukoencephalopathies of non-vascular origin (immunologic-demyelinating, metabolic, toxic, infectious), and (d) inability or refusal to undergo MRI scanning.

The baseline evaluation included brain MRI and thorough medical, functional, and neuropsychological assessments. The clinical assessments were repeated in 12-month intervals at three subsequent follow-up evaluations.

To allow for a valid comparison between subjects/centers, the MRI sequences obtained in each center had to be the same, and each patient had to have three sequences available, without major artifacts. The 78 subjects included in this study did not differ from the complete LADIS cohort in age, sex, baseline Mini-Mental State Examination (MMSE) score, or WML volume, but they had significantly higher education (9.3 vs. 11.7 years; $t = -4.6$, $p < 0.001$).

The study was approved by the Ethics Committees of each participating center in the LADIS study (LADIS Study Group, 2011). All subjects received and signed an informed written consent. The collaborators of the LADIS study are listed in the Appendix II.

Abbreviations: DC, discriminative clustering; FLAIR, fluid-attenuated inversion recovery; LADIS, Leukoaraiosis and Disability Study; MMSE, Mini-Mental State Examination; MRI, magnetic resonance imaging; SVD, small vessel disease; VADAS, Vascular Dementia Assessment Scale–Cognitive Subscale; V_{DC33} , volume of voxels containing small proportion of lesion; V_{DC66} , volume of voxels containing intermediate proportion of lesion; V_{DC100} , volume of voxels containing complete proportion of lesion; $V_{DCHARD} = V_{DC100} + V_{DC66}$; V_{FLAIR} , WML volume as measured with conventional semi-automated analysis on FLAIR images; WML, white matter lesion.

MRI Acquisition and Standard Volume Assessment

All axial MRI scans used were acquired with 1.5T equipment, following the same protocol at each center, including magnetization transfer images (TE = 10–14 ms, TR = 740–780 ms), T2-weighted fast spin echo images (TE = 100–120 ms, TR = 4000–6000 ms), and fluid attenuated inversion recovery (FLAIR) images (TE = 100–140 ms, TR = 6000–10000 ms, TI = 2000–2400 ms). All sequences had a voxel size of $1 \times 1 \times 5\text{--}7.5 \text{ mm}^3$, FOV = 250 and an interslice gap of 0.5 mm.

The extent of hyperintensities on white matter regions including the infratentorial region was evaluated on axial FLAIR images with a semi-automated volumetric analysis (V_{FLAIR}) using a Sparc 5 workstation (SUN) (van Straaten et al., 2006). Lesions were marked and borders were set on each slice using local thresholding (home-developed software Show_Images, version 3.6.1). No distinction was made between subcortical and periventricular hyperintensities. Areas of hyperintensity on T2-weighted images around infarctions and lacunes were disregarded. The number of lacunes was recorded in the white matter and in the deep gray matter using a combination of FLAIR, magnetization prepared rapid-acquisition gradient-echo, and T2 images to distinguish lacunes from perivascular spaces and microbleeds (Gouw et al., 2008). In addition, brain atrophy was rated according to a template-based rating scale on FLAIR images separately on cortical and subcortical regions (Jokinen et al., 2012).

Image Preprocessing

To guarantee that the multispectral information contained in each voxel originated from the exact same location in each subject, intra-patient registration was applied for all sequences available, using the SPM5 toolbox (Friston, 2003), and applying an affine transformation with the lowest resolution image, typically FLAIR, as the template. Furthermore, extra-meningeal tissue voxels were masked out, using a standard automatic method (BET2) (Smith et al., 2004).

Discriminative Clustering Tissue Segmentation

Recent advances in machine learning techniques have shown competitive results in tissue segmentation, often overcoming the accuracies achieved by classic region-growing or threshold-based methods (Styner et al., 2008). In particular, when compared to manual delineation, they are more robust and less subjective. The tissue segmentation method used in this study was such a machine learning technique, based on a data-driven self-supervised methodology, rooted on a DC strategy (Gonçalves et al., 2014). Similar to unsupervised clustering algorithms, such as k-nearest neighbors, DC groups input data according to their multi-dimensional gray level distributional information. In the current study, those distributions were three dimensional, which correspond to the total number of sequences used. The major asset of DC is its ability to use a small set of labeled information to support the clustering assignment. This feature leads to a clear improvement of the segmentation results,

beyond traditional clustering techniques (Gonçalves et al., 2014).

The overall goal of DC can then be summarized as to partition the data space into clustered regions with rather uniform distributions throughout, and consistent label information for all voxels belonging to each cluster. A more detailed explanation is given in Appendix I, with the full mathematical description presented in Gonçalves et al. (2014).

Partial Volume Estimation

DC gives the probability of membership of each voxel to all tissue classes, allowing for the estimation of partial volume information. Since we intended to focus our study on lesioned voxels, we only analyzed those where the proportion of lesion tissue present is relevant.

In this study, three different lesion categories were identified, leading to a corresponding amount of volume estimation: the volume of voxels that have a HIGH (V_{DC100}), INTERMEDIATE (V_{DC66}), or SMALL (V_{DC33}) probability of being lesion. V_{DC100} and V_{DC66} are the volumes where the main tissue in the voxels therein, has a probability of being lesion of $>66\%$ and $<66\%$, respectively. Since both volumes V_{DC100} and V_{DC66} contain a majority of lesion tissue, V_{FLAIR}^1 can be approximated by the sum: $V_{\text{FLAIR}} \approx V_{\text{DCHARD}}^2 \geq V_{\text{DC100}} + V_{\text{DC66}}$. Hence, using DC, the best possible estimate of the volume of visible lesion is attained by V_{DCHARD} . The last category, V_{DC33} corresponds to the volume of voxels where lesion is the second most probable tissue type, with probabilities $\geq 33\%$. Note that, this volume is not considered as lesion in normal segmentation methods, such as the one estimating V_{FLAIR} , since lesion is never the main tissue type therein.

The ability of the present segmentation method to detect early-stage lesions was verified in a subgroup of patients ($n = 19$) with follow-up MRI data, *c.f.* Supplementary Materials: Appendix I). There we show that small partial WML volumes indicate possible future locations of fully developed lesions.

Neuropsychological Evaluation

The cognitive test battery of the LADIS study included the MMSE (Folstein et al., 1975), the Vascular Dementia Assessment Scale–Cognitive Subscale (VADAS) (Ferris, 2003), the Stroop test (MacLeod, 1991), and the Trail making test (Reitan, 1958). For the present purposes, we used the MMSE and VADAS total scores as global measures of cognitive function. In addition, three psychometrically robust compound measures were constituted for the evaluation of specific cognitive domains using averaged standard scores of the individual subtests as described previously (Moleiro et al., 2013): (1) *speed and motor control* = z scores (Trail making A + maze + digit cancellation)/3; (2) *executive functions* = z scores of [(Stroop III-II) + (Trail making B-A) + symbol digit modalities test + verbal fluency]/4; and (3) *memory* = z scores (immediate

¹ V_{FLAIR} , WML volume as measured with conventional semi-automated analysis on FLAIR images.

² V_{DCHARD} , volume corresponding to the voxels where the majority of tissue is lesion.

TABLE 1 | Baseline characteristics of the subjects, $n = 78$.

Characteristic	Values
Age, year, mean (SD)	74.2 (4.8)
Women, n (%)	45 (57.7)
Education, year, mean (SD)	11.7 (4.3)
MMSE score, mean (SD)	27.3 (2.5)
V_{FLAIR} , mm^3 , mean (SD)	23.3 (22.3)
Dice score between V_{FLAIR} and V_{DCHARD} , mean (SD)	70.3 (13.4)
PARTIAL WML VOLUME MEASUREMENTS, CM^3, MEAN (SD)	
V_{DC33} (33%)	3.0 (2.6)
V_{DC66} (66%)	5.1 (5.1)
V_{DC100} (100%)	18.5 (20.6)

MMSE, Mini-Mental State Examination; V_{DC33} , volume of voxels containing small proportion of lesion; V_{DC66} , volume of voxels containing intermediate proportion of lesion; V_{DC100} , volume of voxels containing complete proportion of lesion; $V_{DCHARD} = V_{DC100} + V_{DC66}$; V_{FLAIR} , white matter lesion volume as measured with conventional semi-automated analysis on FLAIR images.

word recall + delayed recall + word recognition + digit span)/4.

The proportion of missing values in neuropsychological test variables varied between 0 and 6.4% at baseline, and between 24.4 and 32.1% at the last follow-up evaluation. This loss of data was due to subjects' death ($n = 2$), drop-out from the follow-up neuropsychological assessments (last year visit, $n = 17$), or inability to complete the entire test battery ($n = 6$).

Statistical Analysis

The predictors of longitudinal cognitive performance were analyzed using linear mixed models (restricted maximum likelihood estimation), which are able to deal with missing values and complex covariance structures. The assessment year (baseline, 1st, 2nd, and 3rd) was used as a within-subject variable, and unstructured covariance structure was adopted. The cognitive test scores were set as dependent variables. The partial lesion volumes (V_{DC33} , V_{DC66} , and V_{DC100}) were tested as predictors, one by one. In all models, age, sex, and years of education were used as covariates. The models were repeated by adding V_{FLAIR} as another covariate, to find out the predictive value of the partial volume measurements incremental to that of the conventionally evaluated WML volume. Similarly, study center was added as a potential confounder, but since it had no essential effect on the results, it was left out from the final analyses. Because of skewed distributions possibly compromising the linearity assumption of the mixture models, logarithmic transformation was applied to all three partial volume measurements and V_{FLAIR} . The results were analyzed with IBM SPSS Statistics 22 mixed module. Statistical significance was set at $p < 0.05$ for all the analyses.

RESULTS

Characteristics of the Subjects

The characteristics of the subjects at baseline are given in **Table 1**. According to the revised Fazekas scale, 28 (35.9%)

subjects had mild, 26 (33.3%) moderate, and 24 (30.8%) severe WML.

Partial WML Volumes and other MRI Findings

Table 1 shows the volumes obtained by the conventional segmentation method, the partial lesion volumes estimated by DC, and the Dice similarity coefficient comparing both segmentation methods. **Figure 1** presents a comparison between the original FLAIR image (1A), the conventionally estimated hyperintensity volume, V_{FLAIR} (1B), and the results obtained for partial WML volumes V_{DC100} (1C), V_{DC66} (1D), and V_{DC33} (1E). Frames 1F-1J shows the corresponding images in the zoomed area denoted by the white rectangle of frame 1A. The evolution around the foci of lesion, from fully blown in the center to the intermediate stage and small proportion of lesion at the edges, can be seen in frames 1H-J. Note that the voxels classified as V_{DC33} are not included in V_{FLAIR} , but are indicative of possible locations of future lesions. **Figure 2** shows similar findings on a higher, centrum semiovale level. The DC segmentation procedure used three different sequences (FLAIR, T2, T1). Here, only FLAIR is shown for illustrative purposes.

For the whole dataset used, the three partial WML volume measures correlated significantly with each other: $V_{DC33} * V_{DC66}$ $r = 0.87$; $V_{DC33} * V_{DC100}$ $r = 0.47$; $V_{DC66} * V_{DC100}$ $r = 0.47$ ($p < 0.001$). They also correlated significantly with V_{FLAIR} : V_{DC33} $r = 0.26$ ($p = 0.024$), V_{DC66} $r = 0.26$ ($p = 0.023$), and V_{DC100} $r = 0.87$ ($p < 0.001$), respectively. However, the measures were not significantly associated with presence of lacunar infarcts (no/few/many) or global brain atrophy score (cortical and subcortical) ($p > 0.05$).

Figure 3 identifies the shared and disparate segmentations between the conventional segmentation (V_{FLAIR}), and DC (V_{DCHARD}) for the subject of **Figure 1**. There is a clear overlap between the two segmentations, as shown by the large number of green pixels. For the subject shown in that figure, there is a small difference between V_{FLAIR} and V_{DCHARD} .

Estimating one subject's full tissue classification, using DC on a PC with Intel® Core™ i5-4590 CPU@ 3.30 GHz with 16 GB of RAM, took about 25 min. The estimation of the labels, on said computer, took about 70 min. An improvement of the latter estimation should streamline the procedure significantly.

Partial WML Volumes as Predictors of Cognitive Performance

The relationships between partial WML volumes and longitudinal cognitive performance are summarized in **Table 2**. Linear mixed models adjusted for age, sex, and education showed significant negative associations between V_{DC33} and the compound score for executive functions. Firstly, V_{DC33} was associated with a significant main effect on overall level of executive performance (scores on average across all four temporal assessments). Secondly, the interaction between V_{DC33} and time (assessment year) indicated significant predictive value of V_{DC33} on change in executive performance over the 3-year follow-up. Specifically, higher load of V_{DC33} related to

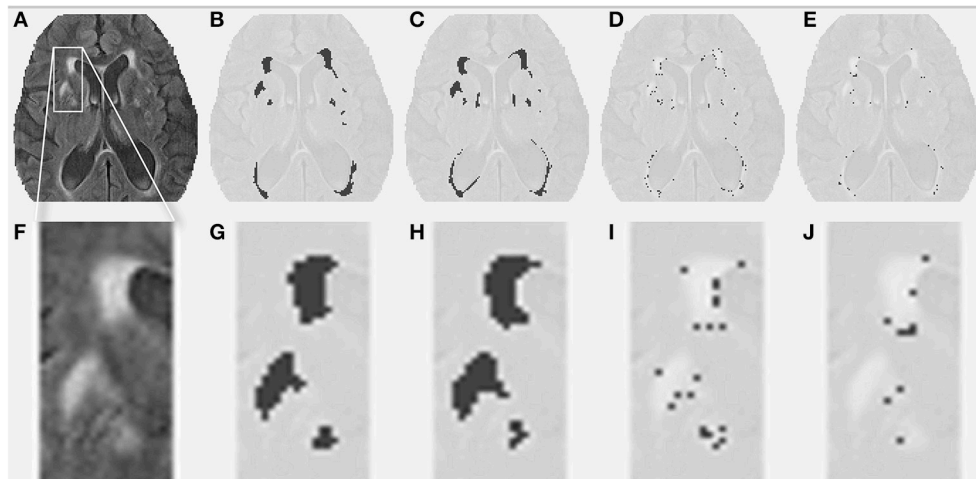


FIGURE 1 | White matter lesions (WML) at a middle level height. (A) FLAIR image for a given subject. **(B)** Conventionally estimated WML. **(C–E)** Estimated WML, using the proposed segmentation algorithm, for full, intermediate, and small proportion of lesion. **(F–J)** Similar images for the zoomed portion depicted by the white box in **(A)**.

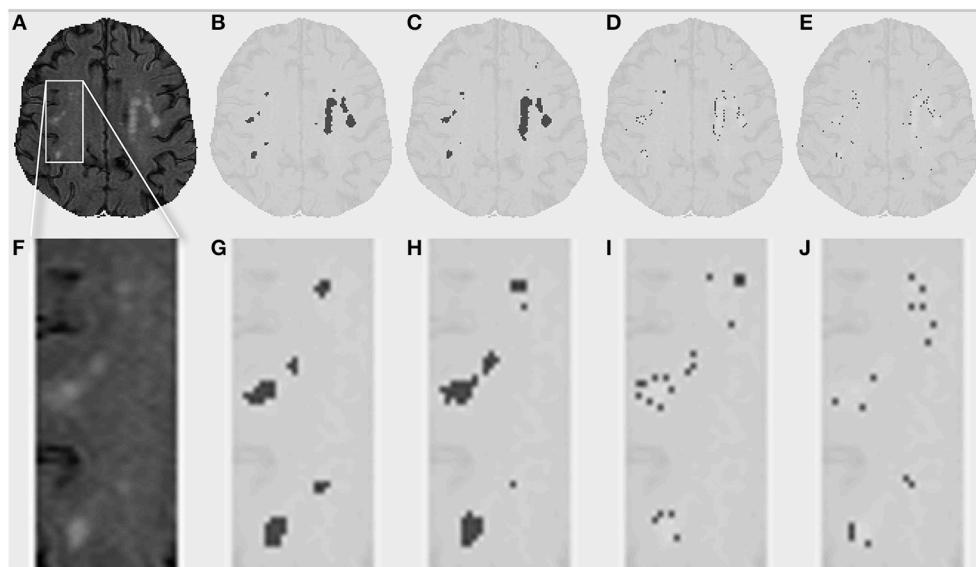


FIGURE 2 | White matter lesions (WML) in the centrum semiovale. (A) FLAIR image for a given subject. **(B)** Conventionally estimated WML. **(C–E)** Estimated WML using the proposed segmentation algorithm, for full, intermediate, and small proportion of lesion. **(F–J)** Similar images for the zoomed portion depicted by the white box in **(A)**.

poorer performance at baseline and steeper decline in executive functions at each subsequent assessment year. After additional adjusting for V_{FLAIR} , these results remained unchanged. Moreover, there was a weak baseline association between V_{DC33} and VADAS total score, but this result was no longer significant after controlling for V_{FLAIR} . V_{DC33} had no significant main effects or interactions with time in MMSE, VADAS, processing speed, or memory functions.

V_{DC66} was related to significant main effects indicating poorer overall level of performance in VADAS and executive functions. Interaction between V_{DC66} and time was significant

only for processing speed. Inspection of the results at individual time points showed a significant baseline association (VADAS, executive functions) as well as longitudinal change by the first (VADAS, executive functions), second (MMSE, executive functions), and the third (executive functions) follow-up year. Controlling for V_{FLAIR} had minimal effect on these results (Table 2).

Finally, V_{DC100} was associated with significant main effects in all neuropsychological scores. V_{DC100}^* time interactions indicated a significant relationship with change during follow-up in four out of five cognitive measures. At this stage, the lesions

TABLE 2 | Relationship between partial white matter lesion volumes and cognitive performance in the 3 year follow-up.

Partial volumes	Cognitive performance				
	MMSE	VADAS	Speed	Executive	Memory
V_{DC33}					
Main effect	ns	ns	ns	12.1 (0.001)**	ns
Volume*time	ns	ns	ns	4.1 (0.011)*	ns
Per year	ns	bl	ns	bl**, 1 yr**, 2 yr**, 3 yr**	ns
V_{DC66}					
Main effect	ns	4.9 (0.030)	ns	12.3 (0.001)**	ns
Volume*time	ns	ns*	3.2 (0.029)*	ns	ns
Per year	2 yr*	bl*, 1 yr**	ns	bl**, 1 yr*, 2 yr*, 3 yr*	ns
V_{DC100}					
Main effect	13.1 (<0.001)**	20.6 (<0.001)**	7.0 (0.010)	28.9 (<0.001)***	4.8 (0.031)*
Volume*time	2.8 (0.047)*	ns	6.5 (0.001)***	5.7 (0.002)**	2.8 (0.050)
Per year	bl, 2 yr**, 3yr*	bl***	bl, 1 yr*	bl***, 1 yr**, 2 yr***, 3 yr***	bl*, 2 yr*, 3 yr*

Linear mixed models adjusted for age, sex, and years of education.

1.Row, main effect *F* (*p*-value) indicates the association between partial lesion volume and mean cognitive performance across all time points.

2.Row, partial lesion volume*time interaction *F* (*p*-value) indicates the association with change of cognitive performance during follow-up.

3.Row, significant association at each time point; bl, baseline, 1 yr/2 yr/3 yr, change per each year compared to baseline (*p* < 0.05).

p* < 0.5, *p* < 0.01, ****p* < 0.001; statistically significant after additional adjustment for *V_{FLAIR}*.

MMSE, Mini-Mental State Examination; ns, non-significant; VADAS, Vascular Dementia Assessment Scale–Cognitive Subscale; *V_{DC33}*, volume of voxels containing small proportion of lesion; *V_{DC66}*, volume of voxels containing intermediate proportion of lesion; *V_{DC100}*, volume of voxels containing complete proportion of lesion; *V_{FLAIR}*, white matter lesion volume as measured with conventional semi-automated analysis on FLAIR images.

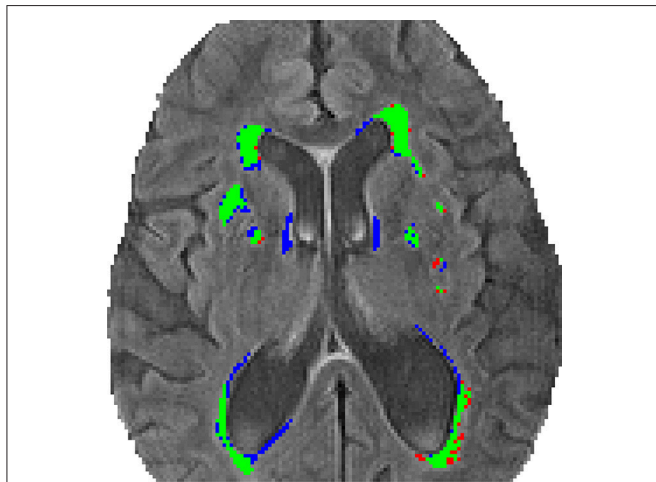


FIGURE 3 | Comparison of the segmentation methods. This image shows the segmentation obtained using the semi-automated volumetric analysis (*V_{FLAIR}*) and the discriminative clustering (*V_{DCHARD}*) for the subject of **Figure 1**. The regions depicted in green correspond to the overlapping segmentation between both approaches. In red are shown regions classified as lesion only by the conventional method, while blue corresponds to voxel classified as lesion only by DC.

were systematically associated with cognitive performance already at baseline. Moreover, steeper decline of performance was evident from the first to the last follow-up evaluation with some variation in different cognitive measures. Most of these results remained even after additional controlling for *V_{FLAIR}* despite its high correlation with *V_{DC100}* (**Table 2**).

Despite *V_{DC33}* and *V_{DC66}*, *V_{FLAIR}* remained a significant predictor on overall performance over the follow-up period

in VADAS and executive functions. However, *V_{FLAIR}* had no independent predictive value incremental to that of *V_{DC100}* on any of the cognitive measures.

DISCUSSION

This study examined the longitudinal cognitive impact of partial WML, from the faintest changes in normal-appearing white matter to the fully developed lesions. The investigation used a novel self-supervised multispectral MRI tissue segmentation method based on DC (Gonçalves et al., 2014) and annually repeated neuropsychological evaluations in 3-year follow-up. Different tissue types were identified utilizing all available MRI sequences simultaneously. WML was then categorized according to partial volumes as small, intermediate, and complete lesion.

Unlike conventional manual tissue segmentation, where the decision is based on an implicit gray level threshold, the proposed method gives access to “under-the-threshold” information regarding lesions. This allows for a better assessment of the lesion progression (qualitative information), as well as sub-voxel volumetry (quantitative information). Other methods exist that provide information about tissue proportions (Van Leemput et al., 2003; Manjón et al., 2010). Yet, they use certain priors that make them unsuitable for WML detection, such as the assumption that one voxel may not contain more than two tissue types.

The main finding of the present study was that even the smallest partial WML volume, *V_{DC33}*, was significantly associated with poorer executive performance already at baseline and predicted future decline in executive functions over the 3-year follow-up. This effect was independent from demographic

factors and, notably, also from the conventionally evaluated hyperintensity volume on FLAIR images. In a subgroup of subjects, we additionally showed that V_{DC33} likely represent the earliest changes in normal-appearing white matter, as their detection, at baseline, indicated future locations of the fully developed lesions after follow-up (Appendix I).

The intermediate stage lesions, V_{DC66} , were independently associated with more extensive cognitive decline, including changes in processing speed and executive functions, as well as global cognitive functions. Moreover, the full-blown lesions, V_{DC100} , were related to even more pronounced effects spreading to all evaluated cognitive domains, both at baseline and in follow-up. It is not surprising that V_{DC100} is a strong predictor of cognitive decline. Since V_{DC100} was highly correlated with V_{FLAIR} , which has previously shown a strong association with cognitive change (Jokinen et al., 2011; Kooistra et al., 2014), it should hold rather similar predictive power.

The novel and most important outcome of the present research is that the volume of lesions detected below the decision threshold already allow for the prediction of particular cognitive scores. The earliest signs of cognitive decline were found specifically in executive functions, which are assumed to essentially rely on the integrity of the prefrontal-subcortical connections of the white matter (O'Sullivan et al., 2001). Executive functions include cognitive control processes such as mental flexibility, inhibition, and planning related to complex goal-directed behavior. These functions are crucial to an individual's functional abilities in everyday life (Tomaszewski Farias et al., 2009).

The results presented in this article support the hypothesis that WML hyperintensities only represent "a tip of the iceberg," while in fact white matter damage in SVD evolves as a gradual process affecting wider areas of the brain (Schmidt et al., 2011; Maillard et al., 2013). Diffusion imaging studies have shown that subtle microstructural changes, even in the normal-appearing brain tissue, are related to cognitive impairment and predict poor cognitive and clinical outcome in follow-up (Schmidt et al., 2010; Jokinen et al., 2013). Microstructural integrity is particularly reduced in the proximity of WML, as shown by fractional anisotropy (Maillard et al., 2011). This phenomenon called "WMH penumbra" may be related to the early-stage partial WML volumes observed in our study. Yet, early onsets of lesion may also occur at some distance from the fully developed WML, as illustrated in detail in Appendix I. To our knowledge, the relationship of these subliminal focal changes with cognitive outcome has not been shown before.

The present sample consists of a mixed group of older subjects, equally stratified to all WML severity degrees, from mild to severe. The participants were recruited in different settings, on the basis of varied referral reasons, representing the diversity of patients with WML encountered in clinical practice (LADIS Study Group, 2011). This heterogeneity of the subjects may, however, obscure the most subtle effects between imaging findings and cognitive decline. Typically to longitudinal studies on aging and cerebrovascular disease, some data was lost because of subjects' dropout from follow-up or inability to complete the entire evaluations.

As a limitation, the LADIS imaging protocol was not initially designed for the present quantitative segmentation method, so only a part of the original imaging data could be utilized. Furthermore, image noise, resolution and movement artifacts are all factors that may influence the outcome of a multicenter study like the one presented here. This is especially true when dealing with partial volume effects. In spite of these limitations, and after correcting for some of the aforementioned confounding factors, we were able to detect subtle indications of lesion progression, based on voxels with a small probability of being lesion.

To improve the reliability of the results shown in this manuscript, a larger cohort could have been considered. Due to concerns regarding consistency across centers, and changes in imaging setups at different times, a more strict policy should be used regarding the MRI sequences employed.

The strengths of this study include a novel, robust, self-supervised, and data-driven image analysis method that enables the identification of tissue types, and the quantification of pathological brain changes, at a very early stage, where conventional MRI evaluation would not be useful. The study also benefits from detailed neuropsychological evaluations, carried out at yearly intervals in 3-year follow-up.

In conclusion, early changes in the normal-appearing white matter already give a clue of progressive deterioration and poor cognitive outcome. At this stage, executive functions are primarily affected, but the detrimental effect on cognition becomes more global when the changes gradually develop into full-blown WML, eventually detectable also on conventional MRI tissue segmentation. These results affirm the proposed multispectral MRI tissue segmentation method as a promising tool having additive value in recognizing the risk of SVD and clinically significant progressive cognitive decline.

AUTHOR CONTRIBUTIONS

All authors have made critical revisions of the manuscript for important intellectual content. In addition to that, the most central work of each author for the study was as follows: HJ; Responsible investigator and corresponding author, design and conceptualization of the study, neuropsychological and clinical data acquisition, statistical analysis, and interpretation, drafting and finishing of the manuscript. NG; Responsible investigator, design and conceptualization of the study, developing of the MRI segmentation method, MRI data analysis, drafting, and finishing of the manuscript. RV; Developing of the MRI segmentation method, MRI data analysis, design, and conceptualization of the study. JL; Expertise in statistical analysis and interpretation. FF; Design of the LADIS study, responsible for the MRI methods. RS; Design of the LADIS study, responsible for the MRI methods. FB; Design of the LADIS study, responsible for the MRI methods. SM; Construction of the neuropsychological test battery, neuropsychological and clinical data acquisition. AV; Neuropsychological and clinical data acquisition. DI; Study coordinator, member of the LADIS steering committee, design of the LADIS study. LP; Coordination and design of the LADIS study. TE; Member of the LADIS steering committee, design of

the LADIS study, study conceptualization, and design. HJ and NG contributed equally to this work.

ACKNOWLEDGMENTS

The Leukoaraiosis and Disability Study was supported by the European Union (grant QLRT-2000-00446). The work of HJ was supported by grants from the Clinical Research Institute and the Medical Research Fund of the Helsinki University Central

Hospital, and Ella and Georg Ehrnrooth Foundation. NG was funded by grant number SFRH/BD/36178/2007 from Fundação para a Ciência e Tecnologia.

SUPPLEMENTARY MATERIAL

The Supplementary Material for this article can be found online at: <http://journal.frontiersin.org/article/10.3389/fnins.2015.00455>

REFERENCES

- Ashburner, J., and Friston, K. J. (2005). Unified segmentation. *Neuroimage* 26, 839–851. doi: 10.1016/j.neuroimage.2005.02.018
- Cruz-Barbosa, R., and Vellido, A. (2011). Semi-supervised analysis of human brain tumour from partially labeled MRS information using manifold learning models. *Int. J. Neural Syst.* 21, 17–29. doi: 10.1142/S0129065711002626
- Ferris, S. H. (2003). General measures of cognition. *Int. Psychogeriatr.* 15(Suppl. 1), 215–217. doi: 10.1017/S1041610203009220
- Folstein, M. F., Folstein, S. E., and McHugh, P. R. (1975). Mini-mental state. a practical method for grading the cognitive state of patients for the clinician. *J. Psychiatr. Res.* 12, 189–198. doi: 10.1016/0022-3956(75)90026-6
- Friston, K. (2003). “Statistical parameter mapping. a practical guide,” in *Neuroscience Databases*, ed R. Kötter (New York, NY: Springer), 237–250. Available online at: <http://www.springer.com/us/book/9781402071652>
- Goebel, R., Esposito, F., and Formisano, E. (2006). Analysis of functional image analysis contest data with brainvoyager QX: from single-subject to cortically aligned group general linear model analysis and self-organizing group independent component analysis. *Hum. Brain Mapp.* 27, 392–401. doi: 10.1002/hbm.20249
- Gonçalves, N., Nikkilä, J., and Vigário, R. (2014). Self-supervised MRI tissue segmentation by discriminative clustering. *Int. J. Neural Syst.* 24:1450004. doi: 10.1142/S012906571450004X
- Gouw, A. A., van der Flier, W. M., Fazekas, F., van Straaten, E. C., Pantoni, L., Poggesi, A., et al. (2008). Progression of white matter hyperintensities and incidence of new lacunes over a 3-year period: the Leukoaraiosis and Disability study. *Stroke* 39, 1414–1420. doi: 10.1161/STROKEAHA.107.498535
- Jokinen, H., Gouw, A. A., Madureira, S., Ylikoski, R., van Straaten, E. C., van der Flier, W. M., et al. (2011). Incident lacunes influence cognitive decline: the LADIS study. *Neurology* 76, 1872–1878. doi: 10.1212/WNL.0b013e31821d752f
- Jokinen, H., Lipsanen, J., Schmidt, R., Fazekas, F., Gouw, A. A., van der Flier, W. M., et al. (2012). Brain atrophy accelerates cognitive decline in cerebral small vessel disease: the LADIS study. *Neurology* 78, 1785–1792. doi: 10.1212/WNL.0b013e3182583070
- Jokinen, H., Schmidt, R., Ropele, S., Fazekas, F., Gouw, A. A., Barkhof, F., et al. (2013). Diffusion changes predict cognitive and functional outcome: the LADIS study. *Ann. Neurol.* 73, 576–583. doi: 10.1002/ana.23802
- Kooistra, M., Geerlings, M. I., van der Graaf, Y., Mali, W. P., Vincken, K. L., Kappelle, L. J., et al. (2014). Vascular brain lesions, brain atrophy, and cognitive decline. the second manifestations of arterial disease-magnetic resonance (SMART-MR) study. *Neurobiol. Aging* 35, 35–41. doi: 10.1016/j.neurobiolaging.2013.07.004
- LADIS Study Group (2011). 2001–2011: a decade of the LADIS (Leukoaraiosis And Disability) study: what have we learned about white matter changes and small-vessel disease? *Cerebrovasc. Dis.* 32, 577–588. doi: 10.1159/000334498
- Lawton, M. P., and Brody, E. M. (1969). Assessment of older people: self-maintaining and instrumental activities of daily living. *Gerontologist* 9, 179–186. doi: 10.1093/geront/9.3_Part_1.179
- Lee, J. D., Su, H. R., Cheng, P. E., Liou, M., Aston, J. A. D., Tsai, A. C., et al. (2009). MR image segmentation using a power transformation approach. *IEEE Trans. Med. Imaging* 28, 894–905. doi: 10.1109/TMI.2009.2012896
- MacLeod, C. M. (1991). Half a century of research on the stroop effect: an integrative review. *Psychol. Bull.* 109, 163–203. doi: 10.1037/0033-2909.109.2.163
- Maillard, P., Carmichael, O., Harvey, D., Fletcher, E., Reed, B., Mungas, D., et al. (2013). FLAIR and diffusion MRI signals are independent predictors of white matter hyperintensities. *Am. J. Neuroradiol.* 34, 54–61. doi: 10.3174/ajnr.A3146
- Maillard, P., Fletcher, E., Harvey, D., Carmichael, O., Reed, B., Mungas, D., et al. (2011). White matter hyperintensity penumbra. *Stroke* 42, 1917–1922. doi: 10.1161/STROKEAHA.110.609768
- Manjón, J. V., Tohka, J., and Robles, M. (2010). Improved estimates of partial volume coefficients from noisy brain MRI using spatial context. *Neuroimage* 53, 480. doi: 10.1016/j.neuroimage.2010.06.046
- Moleiro, C., Madureira, S., Verdelho, A., Ferro, J. M., Poggesi, A., Chabriat, H., et al. (2013). Confirmatory factor analysis of the neuropsychological assessment battery of the LADIS study: a longitudinal analysis. *J. Clin. Exp. Neuropsychol.* 35, 269–278. doi: 10.1080/13803395.2013.770822
- Muller, M., Appelman, A. P., van der Graaf, Y., Vincken, K. L., Mali, W. P., and Geerlings, M. I. (2011). Brain atrophy and cognition: interaction with cerebrovascular pathology? *Neurobiol. Aging* 32, 885–893. doi: 10.1016/j.neurobiolaging.2009.05.005
- O’Sullivan, M., Jones, D. K., Summers, P. E., Morris, R. G., Williams, S. C., and Markus, H. S. (2001). Evidence for cortical “disconnection” as a mechanism of age-related cognitive decline. *Neurology* 57, 632–638. doi: 10.1212/WNL.57.4.632
- Pantoni, L., Basile, A. M., Pracucci, G., Asplund, K., Bogousslavsky, J., Chabriat, H., et al. (2005). Impact of age-related cerebral white matter changes on the transition to disability—the LADIS study: rationale, design and methodology. *Neuroepidemiology* 24, 51–62. doi: 10.1159/000081050
- Pham, D. L., and Prince, J. L. (1998). Partial volume estimation and the fuzzy C-means algorithm. *Int. Conf. Image Process.* 3, 819–822.
- Poels, M. M., Ikram, M. A., van der Lugt, A., Hofman, A., Niessen, W. J., Krestin, G. P., et al. (2012). Cerebral microbleeds are associated with worse cognitive function: the rotterdam scan study. *Neurology* 78, 326–333. doi: 10.1212/WNL.0b013e3182452928
- Reitan, R. M. (1958). Validity of the trail making test as an indicator of organic brain damage. *Percept. Mot. Skills* 8, 271–276. doi: 10.2466/pms.1958.8.3.271
- Schmidt, R., Ropele, S., Ferro, J., Madureira, S., Verdelho, A., Petrovic, K., et al. (2010). Diffusion-weighted imaging and cognition in the leukoaraiosis and disability in the elderly study. *Stroke* 41, e402–e408. doi: 10.1161/STROKEAHA.109.576629
- Schmidt, R., Schmidt, H., Haybaeck, J., Loitfelder, M., Weis, S., Cavalieri, M., et al. (2011). Heterogeneity in age-related white matter changes. *Acta Neuropathol.* 122, 171–185. doi: 10.1007/s00401-011-0851-x
- Smith, S. M., Jenkinson, M., Woolrich, M. W., Beckmann, C. F., Behrens, T. E. J., Johansen-Berg, H., et al. (2004). Advances in functional and structural MR image analysis and implementation as FSL. *Neuroimage* 23(Suppl. 1), S208–S219. doi: 10.1016/j.neuroimage.2004.07.051
- Styner, M., Lee, J., Chin, B., Chin, M. S., Commowick, O., Tran, H., et al. (2008). “3D segmentation in the clinic: a grand challenge II: MS lesion segmentation,” *MIDAS Journal, MICCAI 2008 Workshop*. Available online at: <http://hdl.handle.net/10380/1509>
- Tomaszewski Farias, S., Cahn-Weiner, D. A., Harvey, D. J., Reed, B. R., Mungas, D., Kramer, J. H., et al. (2009). Longitudinal changes in memory and executive functioning are associated with longitudinal change in instrumental activities of daily living in older adults. *Clin. Neuropsychol.* 23, 446–461. doi: 10.1080/13854040802360558

- Van Leemput, K., Maes, F., Vandermeulen, D., and Suetens, P. (1999). Automated model-based tissue classification of MR images of the brain. *IEEE Trans. Med. Imaging* 18, 897–908. doi: 10.1109/42.811270
- Van Leemput, K., Maes, F., Vandermeulen, D., Colchester, A., and Suetens, P. (2001). Automated segmentation of multiple sclerosis lesions by model outlier detection. *IEEE Trans. Med. Imaging* 20, 677–688. doi: 10.1109/42.938237
- Van Leemput, K., Maes, F., Vandermeulen, D., and Suetens, P. (2003). A unifying framework for partial volume segmentation of brain MR images. *IEEE Trans. Med. Imaging* 22, 105–119. doi: 10.1109/TMI.2002.806587
- van Straaten, E. C., Fazekas, F., Rostrup, E., Scheltens, P., Schmidt, R., Pantoni, L., et al. (2006). Impact of white matter hyperintensities scoring method on correlations with clinical data: the LADIS study. *Stroke* 37, 836–840. doi: 10.1161/01.STR.0000202585.26325.74
- Wismüller, A., Vietze, F., Behrends, J., Meyer-Baese, A., Reiser, M., and Ritter, H. (2004). Fully automated biomedical image segmentation by self-organized model adaptation. *Neural Netw.* 17, 1327. doi: 10.1016/j.neunet.2004.06.015
- Zhang, Y., Brady, M., and Smith, S. (2001). Segmentation of brain MR images through a hidden Markov random field model and the expectation-maximization algorithm. *IEEE Trans. Med. Imaging* 20, 45–57. doi: 10.1109/42.906424
- Zijdenbos, A. P., Forghani, R., and Evans, A. C. (2002). Automatic pipeline analysis of 3-D MRI data for clinical trials: application to multiple sclerosis. *IEEE Trans. Med. Imaging* 21, 1280–1291. doi: 10.1109/TMI.2002.806283

Conflict of Interest Statement: The authors declare that the research was conducted in the absence of any commercial or financial relationships that could be construed as a potential conflict of interest.

Copyright © 2015 Jokinen, Gonçalves, Vigário, Lipsanen, Fazekas, Schmidt, Barkhof, Madureira, Verdelho, Inzitari, Pantoni, Erkinjuntti and the LADIS Study Group. This is an open-access article distributed under the terms of the Creative Commons Attribution License (CC BY). The use, distribution or reproduction in other forums is permitted, provided the original author(s) or licensor are credited and that the original publication in this journal is cited, in accordance with accepted academic practice. No use, distribution or reproduction is permitted which does not comply with these terms.